Journal of ELECTRICAL ENGINEERING, VOL 73(2022), NO2, 88–98

sciendo

PAPERS

Smart DTC algorithm with automatic torque ripple adjustment

Marko Rosić, Branko Koprivica, Miroslav Bjekić[1]

The paper presents a direct torque control method with possibilities of automatic algorithm modification in terms of torque ripple reduction. The algorithm is based on the conventional switching table with an arbitrary number of discretized voltage levels allowing higher space-voltage resolution and consequently lower torque ripple. The number of available voltage levels can be easily changed and subsequently torque ripple reduced without the need to modify the conventional switching table. Appropriate algorithm modifications leading to torque ripple reduction are automatized, making this kind of control method simple, effective, and suitable for upcoming smart drives in the rapidly growing industry 4.0. Selective back electromotive force compensation can also be part of automatization with the aim to improve the drive dynamics. Experimental validation presented in the paper confirms improvements in torque ripple reduction retaining the simple and time-effective control structure of the induction machine DTC drive.

K e y w o r d s: variable speed drives, direct torque control, AC machines, switching table, automatic algorithm modification, torque ripple reduction, self-tuning

Abbreviations:

cDTC – conventional direct torque control
SVM – space vector modulation
ST–DTC – switching table direct torque control
DVL–DTC – discretized voltage level DTC
EMF – back electromotive force
DSP – digital signal processor
SVPWM – space vector pulse width modulation
ISR – interrupt service routine

Nomenclature:

L_m – machine mutual inductance
L_s, L_r – stator and rotor inductance
Ψ_s, Ψ_r – stator and rotor flux vector
p – number of pole pairs
T_e – electromagnetic torque
$D\psi, D_T$ – flux and torque demand
T_{ba} – torque band amplitude
k – number of the sector in the $\alpha\beta$ plane
i – number of torque comparator levels
n – number of discretized voltage vector levels
ω – motor speed
u_s, u_{add} – stator voltage and additional (comp.) voltage
$u_{\alpha s}, \psi_{\alpha s}, \psi_{\alpha r}$ – α axis component of stator voltage and stator and rotor flux respectively
$u_{\beta s}, \psi_{\beta s}, \psi_{\beta r}$ – β axis component of stator voltage and stator and rotor flux respectively
$\mathcal{U}$ – resulting voltage vector,
t_s – switching time
t_1, t_2, t_0 – duty cycle of first, second, and zero voltage vector respectively.

1 Introduction

Principles of conventional Direct Torque Control (cDTC) based on lookup switching table are well known and presented in numerous scientific literature [1]. Advantages of direct torque control such as simplicity and great dynamics characteristics are responsible for often implementation of this type of control in modern industrial drives.

Compared to the DTC methods which use some of the space vector modulation (SVM) techniques [2], the cDTC is characterized by high dynamics of the regulated torque response, simpler mathematical calculation, and lower processor burden. However, the high torque ripple, characteristic to control methods that use switching tables, remains very noticeable and dependent on the number of available voltage levels. A huge research effort has been put into solving this shortcoming, from which many cDTC modifications have been born. Some of them went in the direction of modification of switching tables and flux and torque controllers [3]. The second group of modifications moved in the direction of defining a larger number of available voltage levels [4, 5], which was supposed to provide a better spatial resolution of the voltage vector and thus the reduction of the torque ripple. A special way to increase the voltage vector resolution in DTC was provided by the implementation of multilevel inverters [6, 7]. Also, the introduction of multiphase machines and corresponding power converters [8, 9] enabled a further reduction of the torque ripple and an improvement of fault-tolerant characteristics of the cDTC-based drive.

All stated modifications have inevitably influenced the complexity of the original cDTC by further prolonging calculation time and overall processor burden to a greater

[1] University of Kragujevac, Faculty of Technical Sciences Čačak, Serbia, marko.rosic@ftn.kg.ac.rs, branko.koprivica@ftn.kg.ac.rs, miroslav.bjekic@ftn.kg.ac.rs

https://doi.org/10.2478/jee-2022-0012, Print (till 2015) ISSN 1335-3632, On-line ISSN 1339-309X

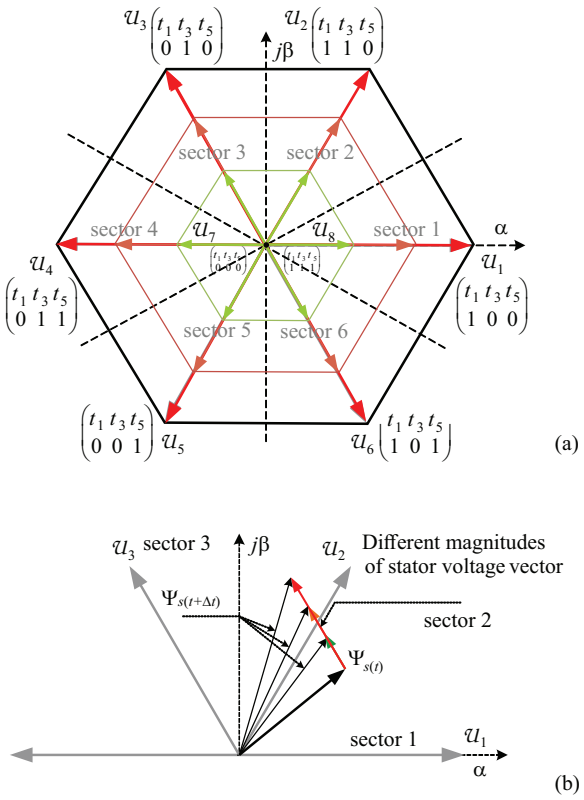

Fig. 1. (a) – $\alpha\beta$ plane resolution of DVL, and (b) – DVL influence on torque increment in next switching cycle

or lesser extent. Algorithms based on switching tables demand changes and expansion of switching tables depending on the number of available voltage levels. Thereby, for any new change in the voltage vector resolution, it is necessary to define a new switching table, *ie* , to define a new and usually more complex algorithm often dependent on motor speed [10–13].

On the other hand, for the realization of a high-quality controlled drive (especially senseless drive) control algorithms demand knowledge of the machine parameters that are prone to slight variation during the drive operation. Online machine parameters estimation [14], self-tuning methods [15], advanced flux estimators [16], state observers [17], dead time compensation [18], *etc* are all part of embedded control algorithms in nowadays drives. These accompanying algorithms improve drive control quality and stability during the operation under various regimes and speeds. To be executed, these components require additional execution time within one scan cycle ($t_s \approx 50$–$100\,\mu$s) on digital platforms. Accordingly, the basic control algorithm must be mathematically simple and less time-consuming as possible.

Upcoming industry 4.0 also requires the development of smart drives that will be able to perform self-evaluation, condition monitoring, life assessment, fault autodetection, auto-modification, *etc*, to reduce down-time and disrupted production. Some of the pioneer examples of these drives are shown in [19–23]. Intelligent diagnosis algorithms of multiple faults in induction motors with a small computation burden are shown in [19–21]. In order to make electric drive robust and fault-tolerant, sensors fault diagnostic algorithms (such as current or speed sensor shown in [22, 23]) should also take a part of the control structure. For this reason, control algorithms must have, on one hand, the ability to quickly modify or optimize during operation depending on the specific needs during the operation, and on the other hand, computational simplicity and efficiency that will leave enough space for implementation of the accompanying compensation algorithms in a time-constrained scenario.

Having said that, there is an emerging need for robust and as simple as possible control algorithms such as cDTC, with high dynamics characteristics and small torque ripple. This paper presents capabilities of a DTC control algorithm based on switching table with possibility of automatic torque ripple adjustment, suitable for implementation in the upcoming smart drives. Reducing the torque ripple is enabled by defining a different number of discretized voltage levels (DVL), which does not require changes in the original switching table. The DVL-DTC method structure is very simple and allows easy self-modification depending on the number of voltage levels defined by the user or by the allowed torque ripple threshold. Moreover, the algorithm leaves the possibility for simple and selective compensation of the back electromotive force (EMF) influence on the torque response quality which will consequently improve the drive dynamics. Control principles and structure of the proposed algorithm can be implemented on multiphase machines as well, further reducing the torque ripple. The execution time of the DVL-DTC algorithm is only a few percent longer than the cDTC. This feature leaves enough time to implement the accompanying components of self-tuning algorithms that improve the general characteristic of the electric drive.

In the paper basic principles of the cDTC and DVL-DTC with electromotive force (EMF) compensation is described, together with the structure of the automatic algorithm modification. The experimental results, presented at the end of the paper, substantiate the effectiveness of the automatically modifiable DVL-DTC algorithm.

2 DVL-DTC algorithm theoretical background

Unlike the existing solutions, the DVL-DTC suggests the use of discretized voltage vectors of different levels in each of the six basic directions of a standard two-level voltage inverter as shown in Fig. 1(a). The torque error defines voltage vector which consequently influences the torque increment in the next switching cycle, as it is shown in Fig.1(b).

Depending on the number of defined voltage levels, a corresponding multilevel torque compartor is formed. The flux comparator and switching table remain the same as with the cDTC, Tab. 1, regardless of the number of defined voltage levels. This DVL-DTC feature allows the

Table 1. Switching table – voltage vector selection

D_ψ	D_T		
	1	0	−1
1	U_{k+1}	U_7 or U_8	U_{k-1}
1	U_{k+2}	U_7 or U_8	U_{k-2}

number of voltage levels to be easily set or changed without the need to define a new switching table as opposed to [5], [10-13] where new switching table had to be defined with each change in the number of available voltage levels.

Changing the number of available discretized voltage vector levels requires only changing the torque comparator, *ie* defining the appropriate number of its levels.

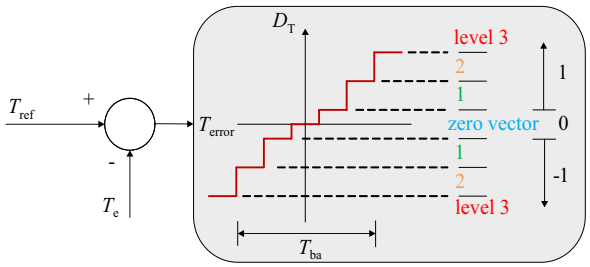

Fig. 2. Hysteresisless 7-level torque comparator

Torque comparator band amplitude T_ba and level limits within can be easily determined (1) according to the number of the set voltage levels n and the original band amplitude T_bac of the torque comparator with cDTC

$$T_\mathrm{ba} = \frac{T_\mathrm{bac}}{3}\, i = \frac{T_\mathrm{bac}}{3}\,(2n+1)\,. \tag{1}$$

The effect of back EMF on torque attenuation at high speeds is documented in [24]. This negative impact of EMF on motor torque can be easily compensated by taking into account an additional voltage vector

$$\begin{aligned} \mathcal{U}_{s\ \mathrm{new}} &= \mathcal{U} + \mathcal{U}_\mathrm{add} \\ &= \mathcal{U}_s + j\omega\boldsymbol{\psi}_s = U_{\alpha s} + jV_{\beta s} + j\omega(\psi_{\alpha s} + j\psi_{\beta s}) \\ &= \underbrace{V_{\alpha s} - \omega\psi_{\beta s}}_{\mathrm{Re}(\mathcal{U}_{s\ \mathrm{new}})} + j\underbrace{(V_{\beta s} + \omega\psi_{\alpha s})}_{\mathrm{Im}(\mathcal{U}_{s\ \mathrm{new}})}\,. \end{aligned} \tag{2}$$

The additional voltage vector must be added to the previously selected voltage level by the multilevel torque comparator, defining the resulting voltage vector that should be applied to stator windings as is shown in Fig. 3. The block diagram of the DVL-DTC algorithm is shown in Fig. 4 where the blocks that differ from the cDTC are highlighted as green.

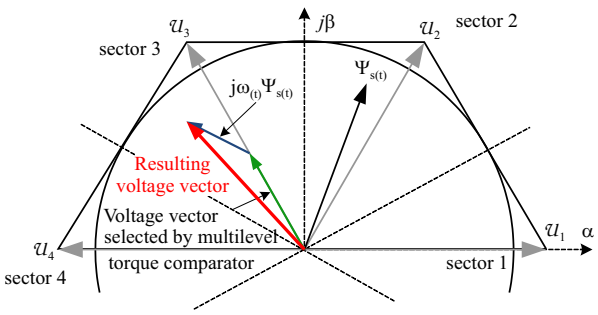

Fig. 3. EMF compensation with added voltage vector

The number of defined voltage vectors can theoretically vary from 2 to the number limited by the DSP processor counter. However, it has been shown that the torque ripple decreases approximately exponentially with increasing the number of voltage levels [25]. Moreover, the torque ripple with only 6 voltage levels decreases almost 8 times compared to the torque ripple with cDTC.

DVL-DTC method can be further expended by the definition of more voltage vector directions. Instead of basic six directions 8, 12, 16 or more voltage directions

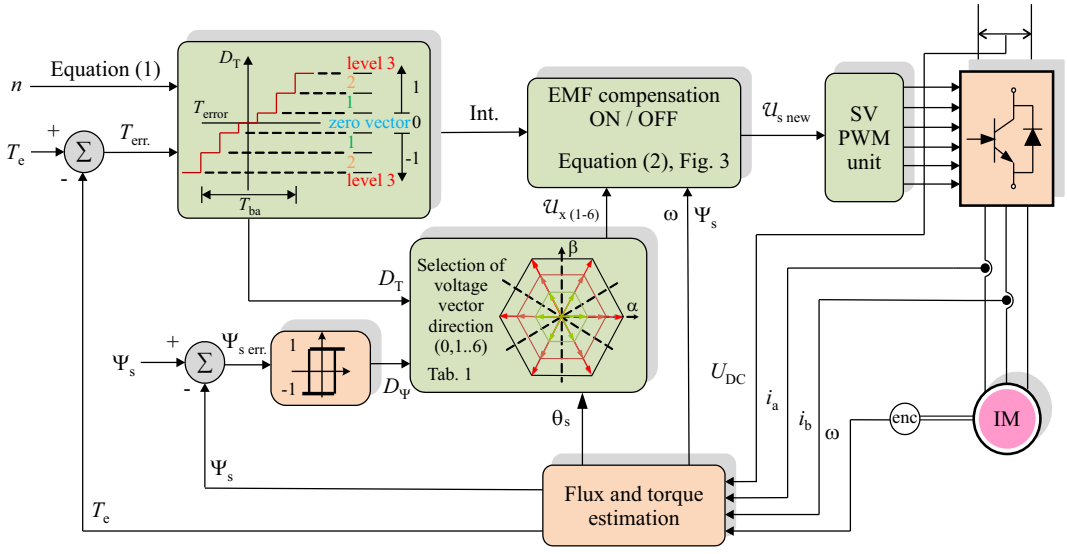

Fig. 4. Block structure of DVL-DTC algorithm

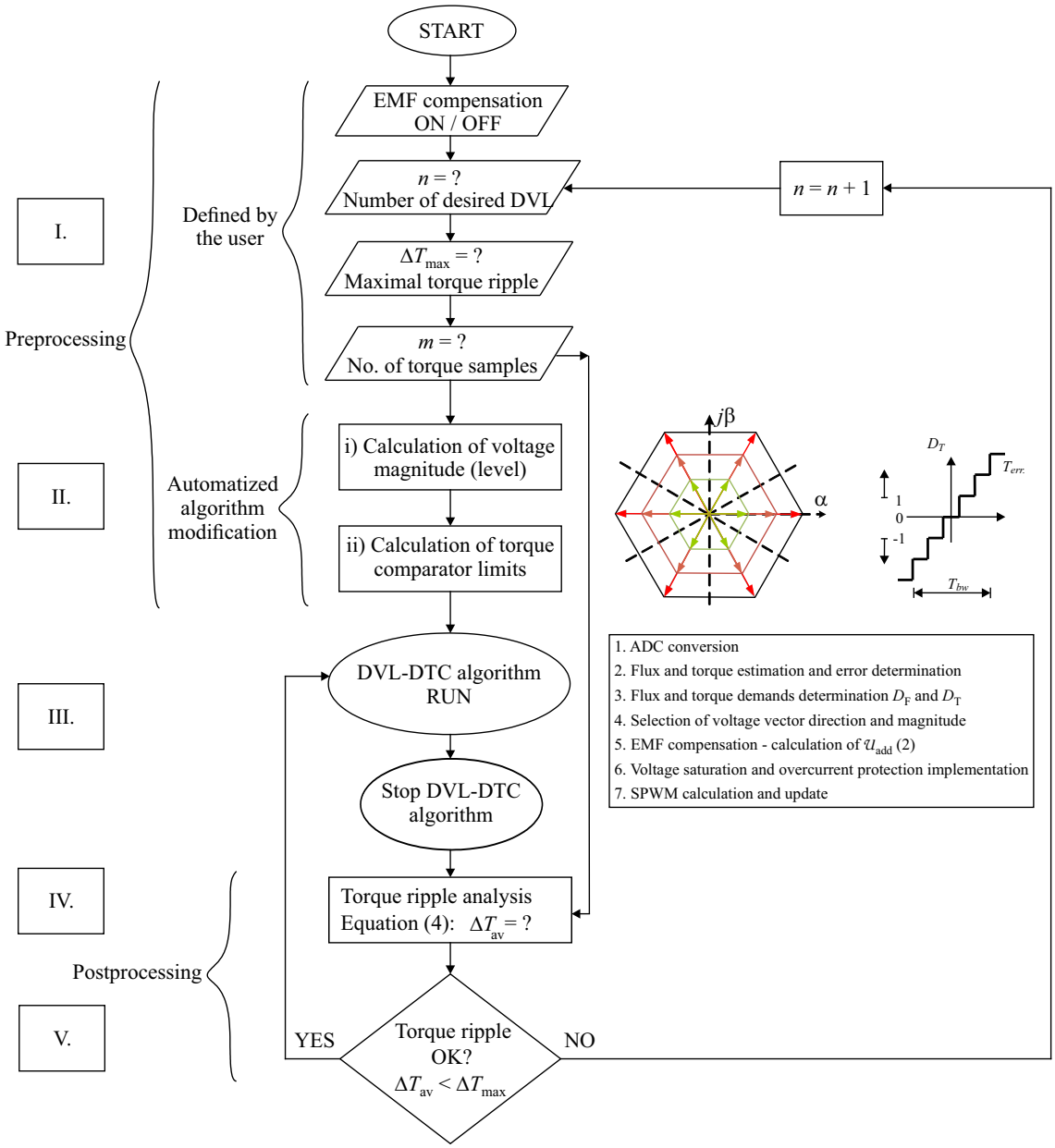

Fig. 5. Smart DVL-DTC algorithm

can be defined which would further reduce the torque ripple. In that case, the algorithm should be modified with new switching tables designed for a higher number of voltage vector directions. However, the results presented in [13] show that the torque ripple reduction degree in the ST-DTC algorithms does not depend on the choice of voltage vectors of different directions to such extent as the choice of vectors of different levels. For that reason, keeping the conventional switching table with 6 basic voltage directions seems justified. Thanks to the absence of coordinate transformations, complex mathematical operations, PI controllers *etc*, the DVL-DTC algorithm has a very short execution time while retaining the high dynamic characteristics for cDTC. The stated characteristics of DVL-DTC appoint it as a very promising candidate for implementation in modern controllers that require a wide torque bandwidth range and control of the allowable torque ripple.

3 Automatic algorithm modification

In order to adequately reduce torque ripple, the number of required discretized voltage levels can be defined in two ways:

- By the user (manually) or,
- Automatically, by the algorithm itself, based on the estimated torque ripple.

The user can choose the number of desired voltage levels as input parameters based on which the DVL-DTC algorithm will further modify its elements before starting the execution of the DVL-DTC algorithm core. On the other hand, the algorithm itself can determine (based on

measuring and analysis of current/torque ripple) whether a further increase in discretized voltage levels (DVL) is required depending on the defined torque ripple limits that may exist during the drive operation. If the torque ripple exceeds the allowed limits, the algorithm will increment the number of voltage levels by one at the next start, based on which the rest of the DVL-DTC algorithm will be modified accordingly. Figure 5 shows the complete algorithm of the DVL-DTC method.

The smart DVL-DTC algorithm is divided into 5 parts. Part I demands a definition of initial drive characteristics such as a starting number of discretized voltage levels and EMF compensation option selection (setting the EMF compensation ON or OFF) by the user. Moreover, values of maximal permissible torque ripple of the drive $\Delta T_{\max}$ and number of estimated torque samples m should be entered as input parameters by the user as well. These values will be used later during the calculation of the resulting torque ripple in part IV and related decision-making criteria in part V of the algorithm in Fig. 5.

As already mentioned, increasing the number of DVL does not demand changes in the switching table (Tab. 1). Further automatized modification of the DVL-DTC algorithm comes down to the next two steps:

(i) Predefining corresponding voltage levels in SVPWM unit and,

(ii) Modification of n-level torque comparator limits.

These two steps defined in parat II represent the main part of automatized adjustment characteristic of the DVL-DTC algorithm. Possibility of simple automatization of these steps is provided thanks to decoupled selection of voltage vector direction (switching table) and voltage vector level (i-level torque comparator) characteristic for DVL-DTC.

Predefinition of appropriate voltage levels implies dividing the full range SVPWM modulated voltage vector into equal parts. For example, if $n = 4$ voltage vectors are defined, the corresponding division will look as it is shown in Fig. 6.

Excluding the overmodulation region and dead time diminishing effect, the maximum value of the voltage vector in SVPWM is limited by the radius of the inscribed circle in the hexagon formed by the basic voltage vectors, which is $86.6\%\,(\sqrt{3}/2)$ of the maximum vector magnitude $(U_1, U_2, \ldots U_6)$. This is further divided into 4 parts defining 4 different levels of voltage in each of six basic directions. The angle α of resulting voltage vector $\mathcal{U}_{\mathrm{s\,new}}$ (as other input parameter of SVPWM unit) in this case, is determined with direction of voltage vector selected by the switching table. This means, in order to apply the resulting voltage vector $\mathcal{U}_{\mathrm{s\,new}}$, SVPWM unit will calculate only times t_1 and t_0 according to well-known equations while t_2 will be zero

$$\begin{aligned}
\mathcal{U}_{\mathrm{s\,new}} &= \mathcal{U}_k \frac{t_1}{t_s} + \mathcal{U}_{k-1} \frac{t_2}{t_s} + \mathcal{U}_0 \frac{t_0}{t_s}\,, \\
t_1 &= \frac{\sqrt{3}\, t_s\, |\mathcal{U}_{\mathrm{s\,new}}|}{U_{DC}} \Big[\cos\alpha \sin\frac{k\pi}{3} - \sin\alpha \cos\frac{k\pi}{3} \Big], \\
t_2 &= \frac{\sqrt{3}\, t_s |\mathcal{U}_{\mathrm{s\,new}}|}{U_{DC}} \Big[-\cos\alpha \sin\big(\frac{k-1}{3}\pi\big) \\
&\qquad + \sin\alpha \cos\big(\frac{k-1}{3}\pi\big) \Big], \\
t_0 &= t_s - t_1 - t_2\,.
\end{aligned} \tag{3}$$

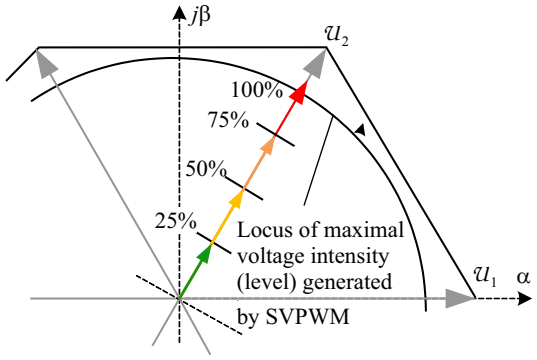

Fig. 6. Definition of different levels of selected vector U_2

On the other hand, if EMF compensation is turned ON, the resulting voltage vector magnitude and angle are determined by the sum of voltage vector chosen by torque comparator and additional compensating voltage calculated by (2). In that case all three times t_1, t_2, and t_0, defining duty cycle of two neighbour basic voltage vectors and zero voltage vector, are calculated respectively.

Appropriate torque comparator band and limits defined within are calculated according to (1) where overall torque band amplitude T_{ba} is divided into corresponding number of levels.

Since in the algorithm described in Fig. 5, parts I and II are done before the core of the DVL-DTC algorithm starts they are referred to as pre-processing. This enables the DVL-DTC algorithm core (part III) to keep its simplicity and structure similar to conventional DTC. The DVL-DTC algorithm core starts with ADC conversion of stator currents as it is presented in Fig. 5. with steps 1 to 7.

The postprocessing part of the algorithm executes within parts 4 and 5 after the algorithm is stopped. This is related to torque ripple analysis and further decision-making step in part V. If the torque ripple is within defined limits the DVL-DTC algorithm can be started again. Otherwise, the number of available voltage levels should be increased within part I. This loop (from part V to part I) enables an increased number of predefined voltage levels by one, after which the following part II will be modified subsequently. The decision regarding resulting torque ripple and if it satisfies maximal defined torque ripple of the drive ($\Delta t_{\max}$ defined by the user in part I)

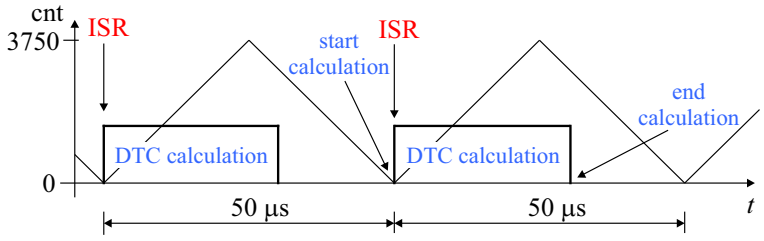

Fig. 7. DSP operation sequence

is made according to calculations of actual average torque ripple defined by

$$\Delta T_{\text{av}} = \sqrt{\frac{1}{m}\sum_{x=1}^{m}(T_x - T_{\text{ref}})^2}$$
$$\Delta T_{\text{av}}(\%) = 100\frac{1}{T_r}\sqrt{\frac{1}{m}\sum_{x=1}^{m}(T_x - T_{\text{ref}})^2}\,. \tag{4}$$

after which the result is compared with $\Delta T_{\max}$ (Fig. 5, part V).

Here m is the number of torque samples (defined by the user in part I) acquired for the purpose of the torque ripple analysis, T_x is the sampled torque value and T_{ref} is the actual torque reference. The average torque ripple ΔT_{av}, and corresponding maximal permissible torque ripple $\Delta T_{\max}$ can be defined as percentage of the torque rated value T_r and subsequently compared, depending on the chosen form of (4) taken into account in part IV. In order to have correctly evaluated average torque ripple ΔT_{av}, the following conditions should be met during the evaluation:

- the EMF compensation should be turned ON, and
- the number of torque samples m in (4) should comprise only torque values during the constant torque reference.

These two conditions eliminate torque error existing when EMF is not compensated and torque error originated from sudden change of torque reference and limited dynamics of the machine torque response, together with a small torque delay due to digital implementation.

Obviously, this loop requires the DVL-DTC drive to be stopped with each iteration until satisfactory demands regarding torque ripple are met. The reason for this lies in the DVL-DTC algorithm parts which are moved in pre-processing and post-processing parts because they do not require to be executed in real-time during the drive operation. On the other hand, this preserves the DVL-DTC algorithm's simplicity. Parts of the algorithm which are moved in pre-processing and post-processing (I, II, IV, and V) are suitable for implementation together with other self-tuning techniques described in the introduction.

However, automatic torque ripple reduction is possible without stopping the DVL-DTC drive in the case when the parts I, II, IV, and V of the algorithm are set to be executed in parallel with part III. This would demand the implementation of these parts in some of the less frequently executed program parts such as speed or position control loop accompanied with DSP with higher processing power. Another way implies its implementation in separate program parts which would be executed on users' demand or other supervisory control applications in parallel processing.

The DVL-DTC algorithm aims to prove its full potential with multiphase machines and corresponding multiphase converters where it can be implemented not disrupting its simplicity. Naturally higher space voltage vector resolution with multilevel converters can be further multiplied by the introduction of DVL. Having said that, without changing the corresponding switching table it will be possible to reduce torque ripple to values characteristic for DTC with continuous voltage vector (SV-DTC, dead-beat DTC, *etc*) where current/torque ripple is limited by the nature of switching modulation techniques. Moreover, implementation of the DVL-DTC method with multiphase converters should improve the characteristic of fault-tolerant drive distinctive for multiphase machines. Implementation and testing the DVL-DTC with multiphase machines, together with implementation of postprocessing part IV and V to be executed in parallel with part III (making the DVL-DTC algorithm completely autonomised) will be the focus of upcoming authors research activities.

4 Experimental setup and results

The DVL-DTC algorithm is implemented and tested on the MSK28335 DSP digital platform in the Laboratory for Electric Machines, Drives, and Automatics at the Faculty of Technical Sciences Čačak. The DSP platform consists of a TMS320F28335 floating-point processor of 150 MHz and a conventional two-level, three-phase inverter with 6 IGBT, 750 W, 310 V DC bus. The platform has serial communication with PC enabling programming, control, and data acquisition through DMC developer pro software. The three-phase induction machine (SIEBER LS71) parameters and other characteristics of the laboratory experimental setup are given in the appendix at the end of the paper (Tab. 2 and Tab. 3).

The sample time frequency is set to 20 kHz, which makes the time frame of $t_s = 50\,\mu$s for DTC algorithm

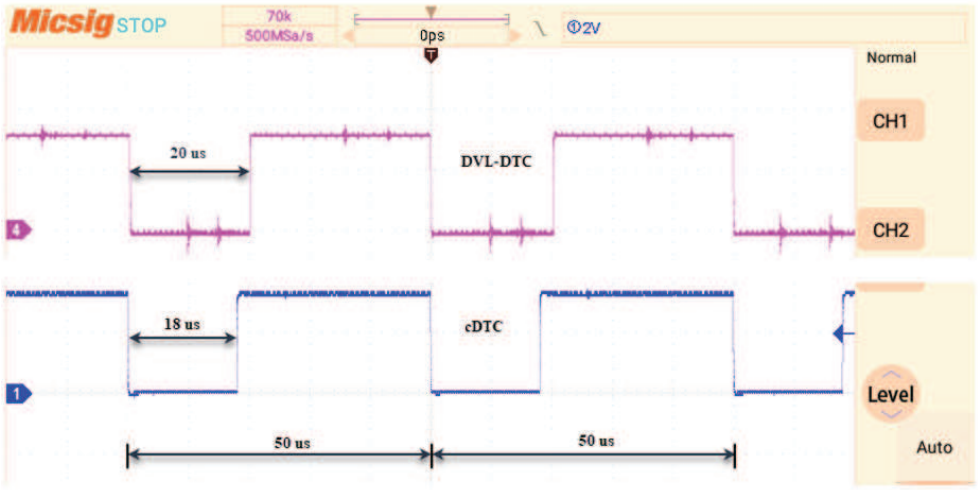

Fig. 8. Calculation times of DVL-DTC (up) and cDTC (down) algorithm core (part III)

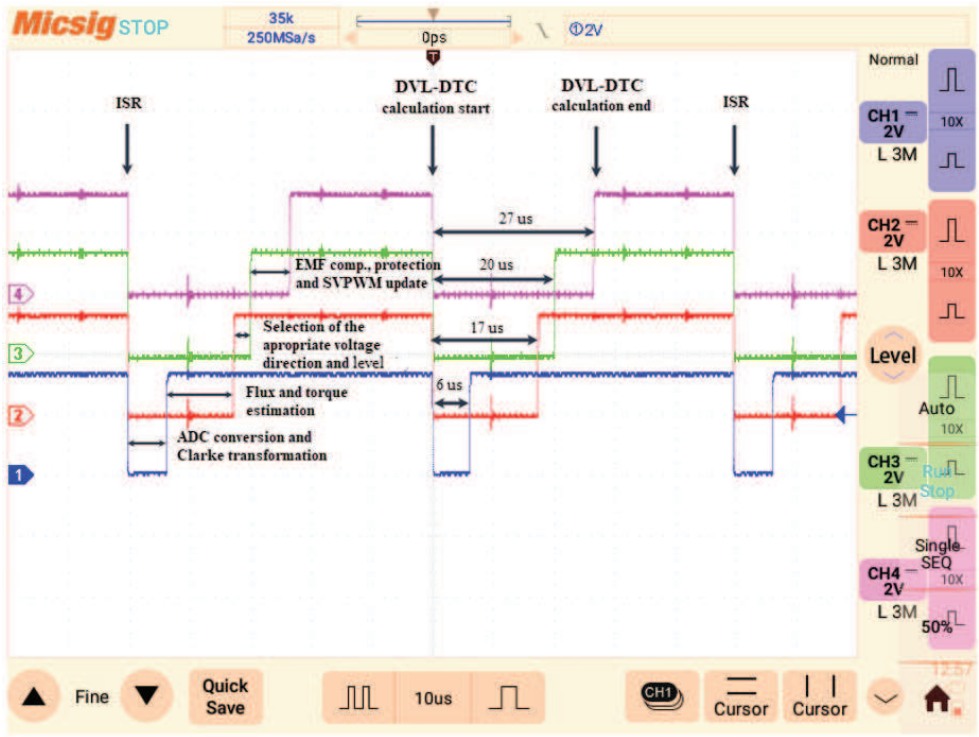

Fig. 9. Calculation times of DVL-DTC (part III) with EMF compensation

execution as it is shown in Fig. 7. Each DTC calculation cycle starts with interrupt service routine (ISR) and ADC conversion and ends with SVPWM update (part III, steps 1 to 7 in Fig. 5).

Flux estimation is realized by Gopinath stile flux observer [26] which combines and exploits the advantage of both voltage and current machine models. Oscilloscope STO1104C is used for recording calculation times of characteristic algorithm parts during the operation. The start and end times of the observed algorithm part are associated with DSP digital outputs. With the start of the characteristic algorithm part corresponding digital output is set to low and at the end is set back to high, which is recorded with the oscilloscope. In order to measure calculation time of DTC algorithm core (part III) a DSP digital output is set to low at the beginning of the algorithm and back to high at the end of the algorithm. Both cDTC and DVL-DTC algorithms were run separately, and subsequently obtained calculation times are compared in Fig. 8. It confirms that the core of the DVL-DTC thanks to its simplicity has about $2\,\mu s$ ($\approx 10\%$) longer calculation time compared to the conventional DTC which makes it one of the simplest DTC techniques. By selection of EMF compensation ON, expression (2) will prolong the over-

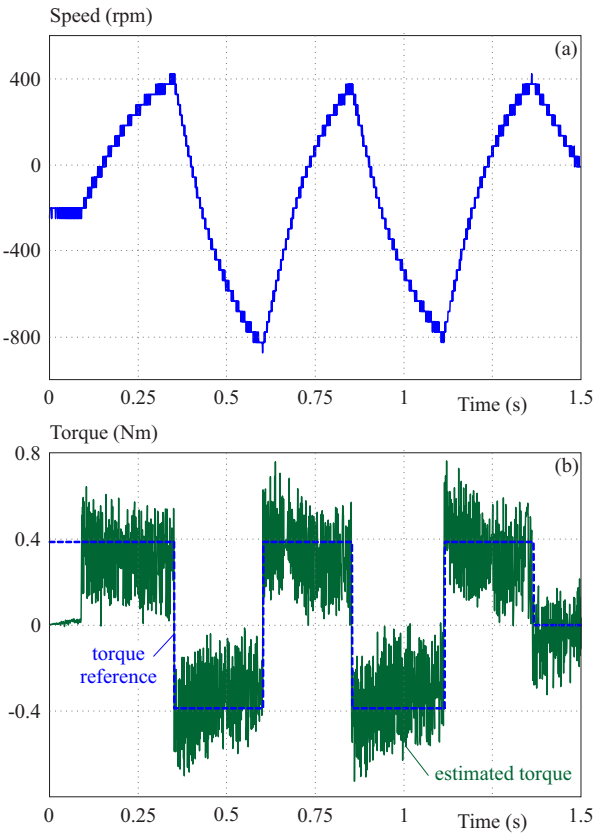

Fig. 10. (a) – speed, and (b) – torque with the cDTC method

all calculation time of part III by 7μs, as is shown in Fig. 9. Moreover, recorded calculation times of other algorithm parts within part III, with back EMF compensation turned ON or OFF are shown as well.

Postprocessing parts IV and V of the DVL-DTC algorithm presented in Fig. 5 were done after the drive is stopped and appropriate average torque ripple calculations (4) are performed subsequently. For proper evaluation of the average torque ripple ΔT_{av} a positive torque reference with corresponding $m = 3000$ torque samples are taken into account with defined $\Delta T_{\max} = 1.5\%$ and EMF compensation turned ON. Obtained experimental results of the DVL-DTC algorithm with 3, 4, 5, and 6 voltage levels are compared with cDTC under the same testing conditions. Results are obtained with unloaded motor and cyclic change in torque reference of ± 0.3 pu. Figure 10 presents the results of motor speed and corresponding torque with the cDTC method where the EMF influence and high torque ripple is evident.

Figure 11 presents the results of the DVL-DTC method, under the same conditions, with different voltage levels, where EMF influence and EMF compensation is turned OFF and ON.

The results presented in Fig. 11 confirm torque ripple reduction with a rise in the number of defined voltage levels. As it can be seen, the negative impact of the EMF on positive torque increments leads to torque steady-state error at higher motor speed. On the other hand, the results show that steady-state torque error is completely eliminated in the case when EMF compensation is enabled (turned ON). Moreover, it can be noted that torque ripple is even smaller in cases where EMF is compensated with the same number of available voltage vector levels. This is expected having in mind that the algorithm chooses higher voltage levels in cases when torque error is high, consequently leading to higher torque ripple.

Nevertheless, the EMF effect, depending on speed and direction of rotation, can be used for improving the torque dynamics. For instance, if the torque reference suddenly decreases during the positive value of the motor speed and torque, the direction of the induced EMF will be such as to support a sudden change of the stator current and consequently shorten torque reversal time. The experimental results of recorded torque reversal with cDTC and DVL-DTC with EMF compensation turned ON or OFF, are presented in Fig. 12.

At the motor speed of 0.5 pu (1500 rpm) sudden change in torque reference of 1 pu (1.3 Nm) is set, while the speed of torque change (torque dynamics) is recorded. Results in Fig. 13, case (a), show that torque reversal time with cDTC is around 300 μs. The torque reversal time with DVL-DTC is around 720 μs in case (b) when EMF is compensated and around 380 μs in case (c), when EMF is not compensated. Noticeably higher dynamics in case (c) speaks in favour of EMF which increases the response speed of the motor torque because the sign of the EMF is such as to support the change of the stator current. The difference in torque response speed in case (a) and case (c) originates from the nature of SVPWM modulation and DC link voltage utilization. Namely, although in a moment of torque transition, when T_{err} has high value and the algorithm chooses a higher available voltage vector, its value is 13% smaller than the basic voltage vector, as it is shown in Fig. 6. Nevertheless, the torque response speed in case (c) is almost two times faster in comparison to the case (b) where EMF compensation is disabled, which significantly contributes to the drive dynamics improvement.

If high dynamic characteristics of the drive are required (high torque and consequently speed and position response), the EMF compensation can be implemented as selective. Namely, the nature of the proposed induced EMF compensation allows no time-consuming implementation (only an if structure) where, in described cases, it can be automatically switched ON or OFF during the motor operation rather than defined by the user in the pre-processing (Fig. 5). These characteristic makes DVL-DTC algorithm autonomous in decision making related to the drive dynamics and torque ripple reduction.

5 Conclusion

The paper presents a smart DTC algorithm based on discretized voltage levels which allow automatic algorithm adaptation depending on torque ripple. Self-adaptation is based on a change of voltage vector resolution that highly influences the torque ripple. The ap-

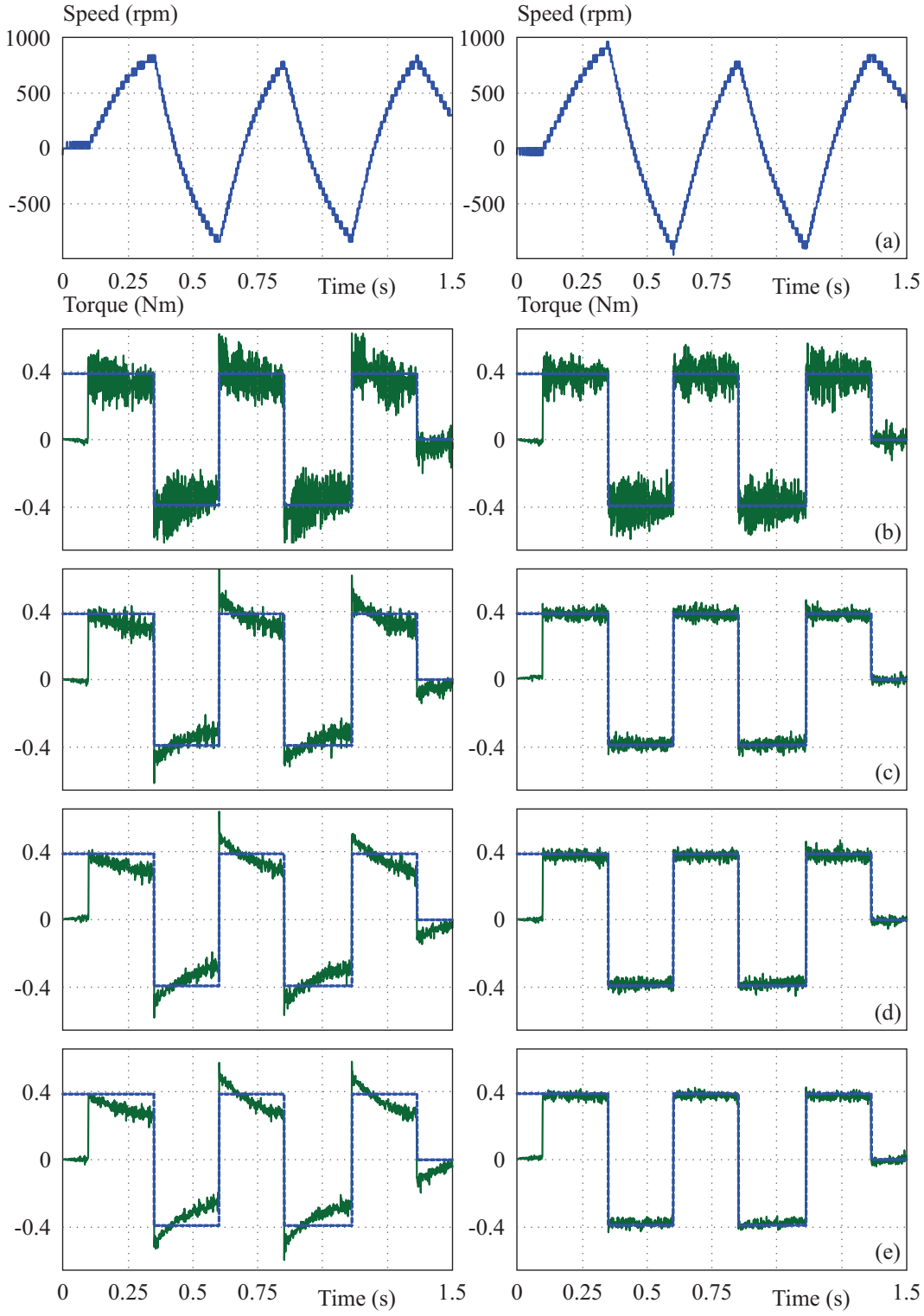

Fig. 11. (a) – speed and torque of DVL-DTC with (b) – 3, (c) – 4, (d) – 5), and (e) – 6 voltage levels and with and without EMF compensation

propriate number of discretized voltage vector levels can be set by the user, or automatically selected based on the permissible torque ripple of the electric drive. The basic simplicity of conventional DTC has been kept, as well as high dynamics of the torque response. Obtained experimental results prove the calculation simplicity of the DVL-DTC in comparison to the conventional DTC and torque ripple reduction with a higher number of discretized voltage levels. Influence and possibilities of selective EMF compensation are also presented through the experimental results which confirm higher torque dynamics in cases when EMF compensation is disabled. Simple

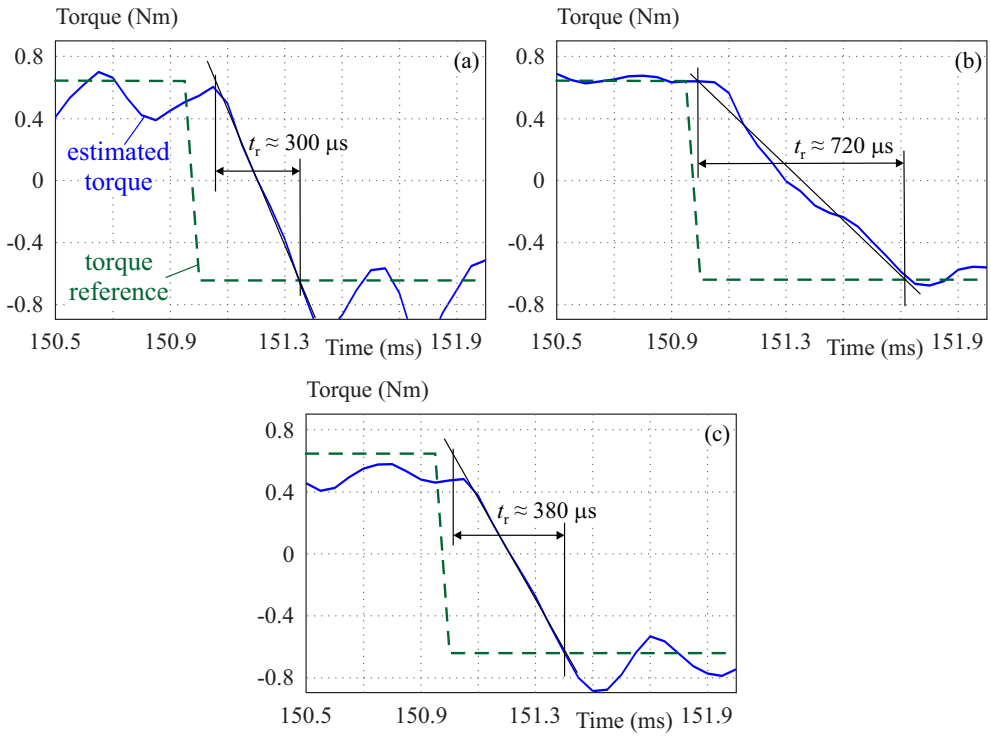

Fig. 12. Torque reversal time at motor speed $w = 1500$ rpm with: (a) – cDTC, (b) – DVL-DTC with EMF turned ON, and (c) – DVL-DTC with EMF compensation turned OFF

implementation of selective EMF compensation and automatic adaptation in terms of torque ripple reduction makes the DVL-DTC algorithm suitable for application in the upcoming smart drives.

Appendix

Table 2. Sieber LS71 motor parameters

U_n (V)	400	$R_s(\Omega)$	24.6
I_n (A)	0.95	$R_r(\Omega)$	16.1
P_n (W)	370	$L_m(H)$	1.46
n_n (rpm)	2860	$L_s(H)$	1.48
p (pp)	1	$L_r(H)$	1.48

Table 3. MSK28335 and oscilloscope

MSK28335 platform	ACPM 750 (W) DSP TMS320F28335
	150 (MHz), 2 ch. 12-bit D/A, JTAG (XDS510/XDS510PP)
	Overcurrent, over/under voltage protection
	DMC developer pro software
Oscilloscope STO1104C	4 channel full, 100 (MHz), 1 (GSa/s), 28 (Mpts)
	8" TFT LCD touch tablet DSO, UART, CAN, LIN, SPI, I2C decoding

Acknowledgements

This study was supported by the Ministry of Education, Science and Technological Development of the Republic of Serbia, and these results are part of the Grant No.451-03-68/2022-14/200132 with University of Kragujevac, Faculty of Technical Sciences Čačak.

References

[1] R. H. Kumar, A. Iqbal, and N. C. Lenin, "Review of recent advancements of direct torque control in induction motor drives – a decade of progress", *IET Power Electronics*, vol. 11, no. 1, pp. 1–15, 2018.

[2] Y. Zhang, J. Zhu, W. Xu, and Y. Guo, "A simple method to reduce torque ripple in direct torque-controlled permanent-magnet synchronous motor by using vectors with variable amplitude and angle", *IEEE Transactions on Industrial Electronics*, vol. 58, no. 7, pp. 2848-2859, 2011.

[3] A. Purcell and P. Acarnley, "Device switching scheme for direct torque control", *Electronics Letters*, vol. 34, no. 4, pp. 412–414, 1998.

[4] I. M. Alsofyani, N. R. N. Idris, K. Lee, and Dynamic, "Hysteresis Torque Band for Improving the Performance of Lookup-Table-Based DTC of Induction Machines", *IEEE Transactions on Power Electronics*, vol. 33, no. 9, pp. 7959–7970, 2018.

[5] D. Casadei, G. Serra, and A. Tani "Implementation of a direct control algorithm for induction motors based on discrete space vector modulation", *IEEE Transactions on Power Electronics*, vol. 15, no. 4, pp. 769–777, 2012.

[6] F. Khoucha, M. S. Lagoun, A. Kheloui, and M. El-H. Benbouzid, "A Comparison of Symmetrical and Asymmetrical Three-Phase H-Bridge Multilevel Inverter for DTC Induction Motor Drives", *IEEE Transactions on Energy Conversion*, vol. 26, no. 1, pp. 64–72, 2011.

[7] D. Mohan, X. Zhang, and G. H. B. Foo, "Generalized DTC Strategy for Multilevel Inverter Fed IPMSMs with Constant Inverter Switching Frequency and Reduced Torque Ripples", *IEEE Transactions on Energy Conversion*, vol. 32, no. 3, pp. 1031–1041, 2017.

[8] L. Zheng, J. E. Fletcher, B. W. Williams, and X. He, "A novel direct torque control scheme for a sensorless five-phase induction motor drive", *IEEE Transactions on Industrial Electronics*, vol. 58, no. 2, pp. 503–513, 2011.

[9] J. K. Pandit, M. V. Aware, R. V. Nemade, and E. Levi, "Direct Torque Control Scheme for a Six-Phase Induction Motor with Reduced Torque Ripple", *IEEE Transactions on Power Electronics*, vol. 32, no. 9, pp. 7118–7129, 2017.

[10] R. E. K. Meesala and V. K. Thippiripati, "An Improved Direct Torque Control of Three-Level Dual Inverter Fed Open-Ended Winding Induction Motor Drive Based on Modified Look-Up Table", *IEEE Transactions on Power Electronics*, vol. 35, no. 4, pp. 3906–3917, 2020.

[11] S. Suresh, P. P. R. "Virtual Space Vector-Based Direct Torque Control Schemes for Induction Motor Drives", *IEEE Transactions on Industry Applications*, vol. 56, no. 3, pp. 2719–2728, 2020.

[12] Y. N. Tatte, M. V. Aware, J. K. Pandit, and R. Nemade, "Performance Improvement of Three-Level Five-Phase Inverter-Fed DTC-Controlled Five-Phase Induction Motor During Low-Speed Operation", *IEEE Transactions on Industry Applications*, vol. 54, no. 3, pp. 2349–2357, 2018.

[13] A. S, M. Thathan "Novel switching table for direct torque controlled permanent magnet synchronous motors to reduce torque ripple", *Journal of Power Electronics*, vol. 13 no. 6, pp. 939–954, 2013.

[14] M. H. Holakooie, M. Ojaghi, and A. Taheri, "Direct Torque Control of Six-Phase Induction Motor with a Novel MRAS-Based Stator Resistance Estimator", *IEEE Transactions on Industrial Electronics*, vol. 65, no. 10, pp. 7685–7696, 2018.

[15] M. N. Uddin, M. Hafeez, and N. A. Rahim, "Self-tuned NFC and adaptive torque hysteresis based DTC scheme for IM Drive", *Proc. of the IEEE Industry Applications Society Annual Meeting*, pp. 1–8, 2011.

[16] W. Xu, R. Dian, Y. Liu, D. Hu, and J. Zhu, "Robust Flux Estimation Method for Linear Induction Motors Based on Improved Extended State Observers", *IEEE Transactions on Power Electronics*, vol. 34, no. 5, pp. 4628–4640, 2019.

[17] J. Li, A. Thapa, and K. A. Corzine, "Speed-sensorless drive for induction machines using a novel hybrid observer", *Proc. of the IEEE Applied Power Electronics Conference and Exposition (APEC*,), pp. 512–517, 2017.

[18] L. Q. Zhou, "A new dead-time compensation method on direct torque control system based on DSP", *Proc. of the 4th IEEE Conference on Industrial Electronics and Applications*, pp. 2359–2362, 2009.

[19] R. H. C. Palácios, W. F. Godoy, A. Goedtel, I. N. d. Silva, D. Morigo-Sotelo, and O. Duque-Perez, "Time domain diagnosis of multiple faults in three phase induction motors using intelligent approaches", *Proc. of the IEEE 11th International Symposium on Diagnostics for Electrical Machines, Power Electronics and Drives (SDEMPED*,), pp. 85–89, 2017.

[20] M. N. S. K. Shabbir, X. Liang, and S. Chakrabarti, "An ANOVA-Based Fault Diagnosis Approach for Variable Frequency Drive-Fed Induction Motors", *IEEE Transactions on Energy Conversion*, vol. 36, no. 1, pp. 500–512, 2021.

[21] S. Shi, Y. Sun, X. Li, H. Dan, and M. Su, "Moving Integration Filter-Based Open-Switch Fault-Diagnosis Method for Three-Phase Induction Motor Drive Systems", *IEEE Transactions on Transportation Electrification*, vol. 6, no. 3, pp. 1093–1103, 2020.

[22] B. Gou, Y. Xu, Y. Xia, G. Wilson, and S. Liu, "An Intelligent Time-Adaptive Data-Driven Method for Sensor Fault Diagnosis in Induction Motor Drive System", *IEEE Transactions on Industrial Electronics*, vol. 66, no. 12, pp. 9817–9827, 2019.

[23] C. D. Tran, P. Palacky, M. Kuchar, P. Brandstetter, and B. H. Dinh, "Current and Speed Sensor Fault Diagnosis Method Applied to Induction Motor Drive", *IEEE Access*, vol. 9, pp. 38660–38672, 2021.

[24] M. Rosic, M. Bjekic, M. Bebic, and B. Jeftenic, "Electromotive force compensation in direct torque control with discretized voltage levels", *Proc. of the 4th International Symposium on Environmental Friendly Energies and Applications (EFEA*,), pp. 1–6, 2016.

[25] M. Rosic, S. Antic, and M. Bebic, "Improvements of torque ripple reduction in DTC IM drive with arbitrary number of voltage levels and automatic algorithm modification", *Turkish Journal of Electrical Engineering & Computer Sciences*, vol. 29, no. 2, pp. 687–703, 2021.

[26] N. T. West and R. D. Lorenz, "Digital Implementation of Stator and Rotor Flux-Linkage Observers and a Stator-Current Observer for Deadbeat Direct Torque Control of Induction Machines", *IEEE Transactions on Industry Applications*, vol. 45, no. 2, pp. 729–736, 2009.

Received 27 January 2022

Marko Rosić was born in Priboj, Serbia, in 1984. He received the BSc and MSc degrees in electrical engineering from the Faculty of Technical Sciences Čačak, the University of Kragujevac in 2008, and the PhD degree from the School of Electrical Engineering, the University of Belgrade in 2016. Since 2008 he has been with the Department of Power Engineering, Faculty of Technical Sciences Čačak, University of Kragujevac, currently as an Associate Professor. He is author or co-author of more than 60 journal and conference papers. His research interests include electrical machines and drives, power electronics, and control of electrical drives.

Branko Koprivica received the PhD degree in electrical engineering from the University of Kragujevac, Kragujevac, Serbia, in 2015. He is currently an Associate Professor with the Department of Electrical and Electronic Engineering, Faculty of Technical Sciences in Čačak, University of Kragujevac. He has authored or coauthored over 70 publications. His current research interests include numerical methods in electromagnetics, magnetism and magnetic measurements, metrology of electrical and nonelectrical quantities, and sensors and remote experiments.

Miroslav Bjekić graduated from the Technical Faculty Čačak (1991), he received his magistrate degree from the University of Belgrade, Department of Electrical Engineering (1996), and his PhD degree from the Technical Faculty Čačak (2006). His field of research includes electric micromachines, simulation, and modelling of electromechanical processes. He is co-author of two university textbooks, author of two handbooks for electric machines laboratory exercises, three computer handbooks, and didactic handbook for engineering teachers. He has created six original educational computer software.